Progression of progenitor B-cell leukemia is associated with alterations of the bone marrow micro-environment

Josefine Åhsberg,[1] Pingnan Xiao,[2] Kazuki Okuyama,[1] Rajesh Somasundaram,[1] Tobias Strid,[3] Hong Qian[2] and Mikael Sigvardsson[1,3]

[1]Department of Clinical and Experimental Medicine, Linköping University, Linköping; [2]Center for Hematology and Regenerative Medicine, Department of Medicine, Karolinska Institute, Karolinska University Hospital, Stockholm and [3]Division of Molecular Hematology, Lund University, Lund, Sweden

Correspondence: MIKAES SIGVARDSSON - mikael.sigvardsson@med.lu.se

doi:10.3324/haematol.2018.214031

Progression of pre-B cell leukemia is associated with alterations of the bone marrow micro-environment.

Josefine Åhsberg[1], Pingnan Xiao[2], Kazuki Okuyama[1], Rajesh Somasundaram[1], Tobias Strid[3], Hong Qian[2] and Mikael Sigvardsson[1,3*].

Supplementary material.

Table S1. Stroma cell populations change gene expression patterns during disease progression. The table consists of excel sheets with gene expression data presented in the heatmap in figure 3 and S3 and the PC-diagram in 4A.

Table S2. Leukemia progression increases the potential communication pathways between mature stroma cells and B-ALL cells. The table consists of excel sheets with defined receptor ligand interactions identified by in silico analysis.

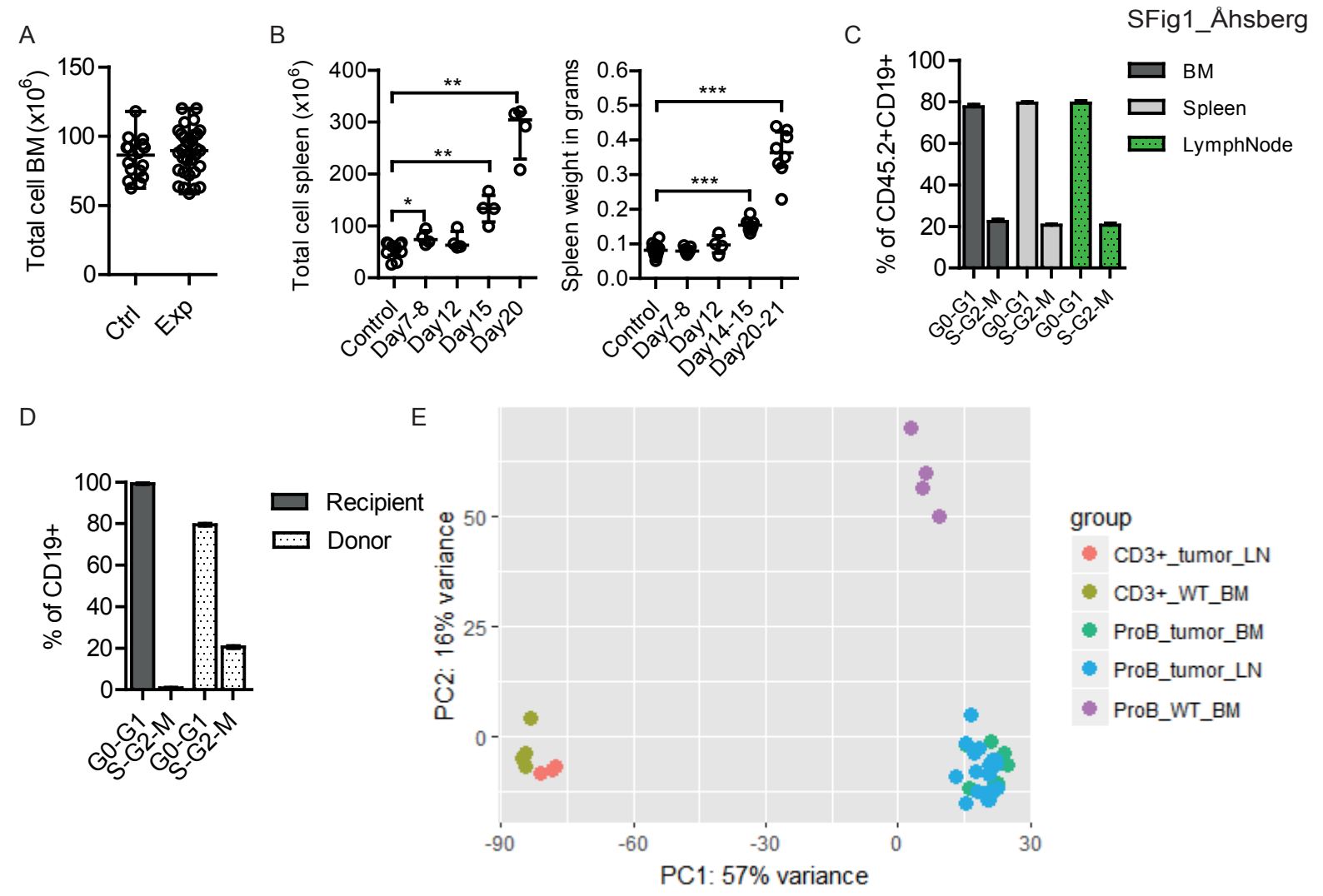
SFig1_Åhsberg
A
Total cell BM (x10^6)
150
100
50
0
Ctrl
Exp
B
Total cell spleen (x10^6)
400
300
200
100
0
**
**
*
Control
Day7-8
Day12
Day15
Day20
Spleen weight in grams
0.6
0.5
0.4
0.3
0.2
0.1
0.0
***
***
Control
Day7-8
Day12
Day14-15
Day20-21
C
% of CD45.2+CD19+
100
80
60
40
20
0
G0-G1
S-G2-M
G0-G1
S-G2-M
G0-G1
S-G2-M
BM
Spleen
LymphNode
D
% of CD19+
100
80
60
40
20
0
G0-G1
S-G2-M
G0-G1
S-G2-M
Recipient
Donor
E
PC2: 16% variance
50
25
0
-90
-60
-30
0
30
PC1: 57% variance
group
CD3+_tumor_LN
CD3+_WT_BM
ProB_tumor_BM
ProB_tumor_LN
ProB_WT_BM

Figure S1. Leukemic Pro-B cells are able to engraft to central as well as peripheral lymphoid organs where they maintain proliferative capacity and overall molecular profile. A) Graph showing the total cellularity of bone marrow from control (n=17) and experimental animals at all time points (n=31) from a total of 3 experiments investigating 3 tumors (806, 887, 889). Error bars are median +/- interquartile range. B) Graph showing the total cell number in spleen controls (n=10) and experiment animals (n=16) as well as spleen weight at indicated time points after iv-injection of 100,000 LN 806 pro-B tumor cells. Each dot represent one mouse and statistical analysis was performed in GraphPad Prism using Mann Whitney test, $p^* = <0.05$, $p^{**} = <0.01$, $p^{***} = < 0.001$. C) Graph displaying the cell cycle status (DAPI) of $CD45.2^+CD19^+$ (1103 donor derived) cells in bone marrow, spleen and lymph node of WT $CD45.1^+$ recipients (n=2). D) Graph displaying the cell cycle status (DAPI) of $CD45.1^+CD19^+$ (recipient) and $CD45.2^+CD19^+$ (1103 donor) cells in spleen WT $CD45.1^+$ recipients (n=2). E) $LIN^-CD19^+CD43^+KIT^+$ (Pro-B) cells and $CD3^+$ (T-cells) were sorted from indicated tissue of *Wt* and leukemic mice, RNA was extracted and subjected to RNA-sequencing. This graph displays a principal component analysis (PCA) of a total of 15342 genes in leukemic mice lymph node $CD3^+$ (n=3), WT mice bone marrow $CD3^+$ (n=4), leukemic mice bone marrow Pro-B (n=8), leukemic mice lymph node Pro-B (n=20) and *Wt* mice bone marrow Pro-B (n=4).

SFig2_Åhsberg

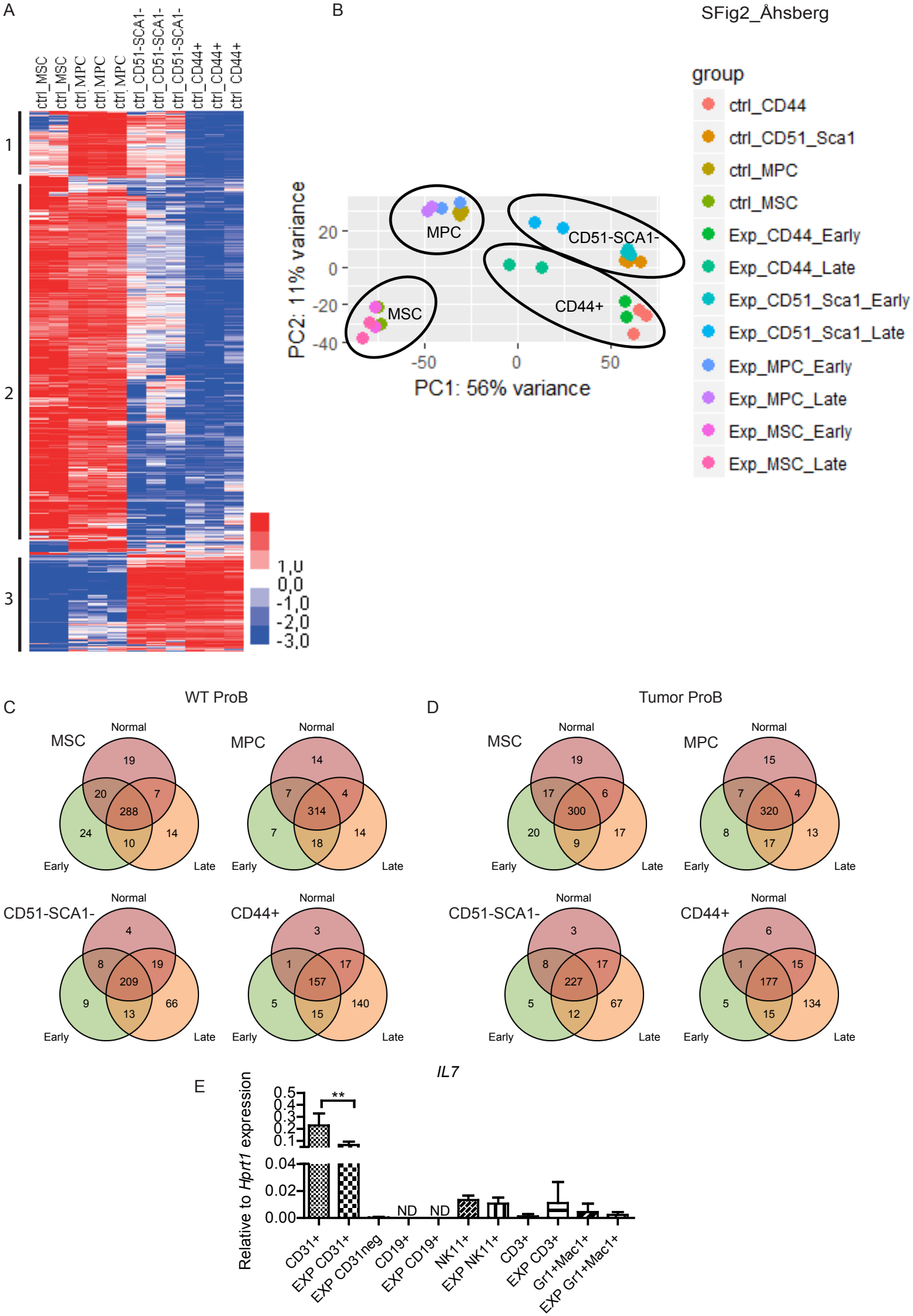

Figure S2. Gene expression in stroma cell populations in the bone marrow are affected by the presence and level of tumor load A) Heat map visualizing RNA-expression in MSC, MPC, $CD51^{-}SCA1^{-}$ and $CD44^{+}$ *Wt* stroma populations. Shown are a total of 2047 genes found to be significantly up- or down regulated in at least one of the cell types in comparison to a mean of means of all four cell types. To be classified as significant, a gene had to be at least 2-fold changed with a false discovery rate (FDR) of <0.05. Numbers 1-3 represent the different clusters analyzed for GO using DAVID. B) Principal component analysis (PCA) of control and experimental stroma populations. Each cell type is circled in the figure, and each time point is represented as a color. Early < day 12 after transplantation, Late > day 15 after transplantation. C-D) Venn diagrams displaying a schematic view of the theoretical interactions between receptors found on *Wt* ProB (©) or B-ALL cells (D), with ligands on *Wt* (normal) and experimental (Early, Late) stroma populations. E) Graph displaying Q-PCR data from spleen of control and transplanted experiment animals (EXP). $MHC1^{+}MHC2^{-}CD31^{+}$ (control n=3 independent sorts from 3 mice, exp n=7 independent sorts from 7 mice), $MHC1^{+}MHC2^{-}CD31^{-}$ (exp n=7), $CD3^{+}$ (control n=2, exp n=2), $CD19^{+}$ (control=2, exp=2), $NK1.1^{+}$ (control=2, exp=2), and $GR1^{+}/Mac1^{+}$ (control=2, exp=4). Figure indicates the fold expression of *Il7* relative to *Hprt* in each population. Each independent sample were analyzed by Q-PCR in triplicate. Statistical analysis was performed in GraphPad Prism using unpaired t-test, p^{**}= <0.01.

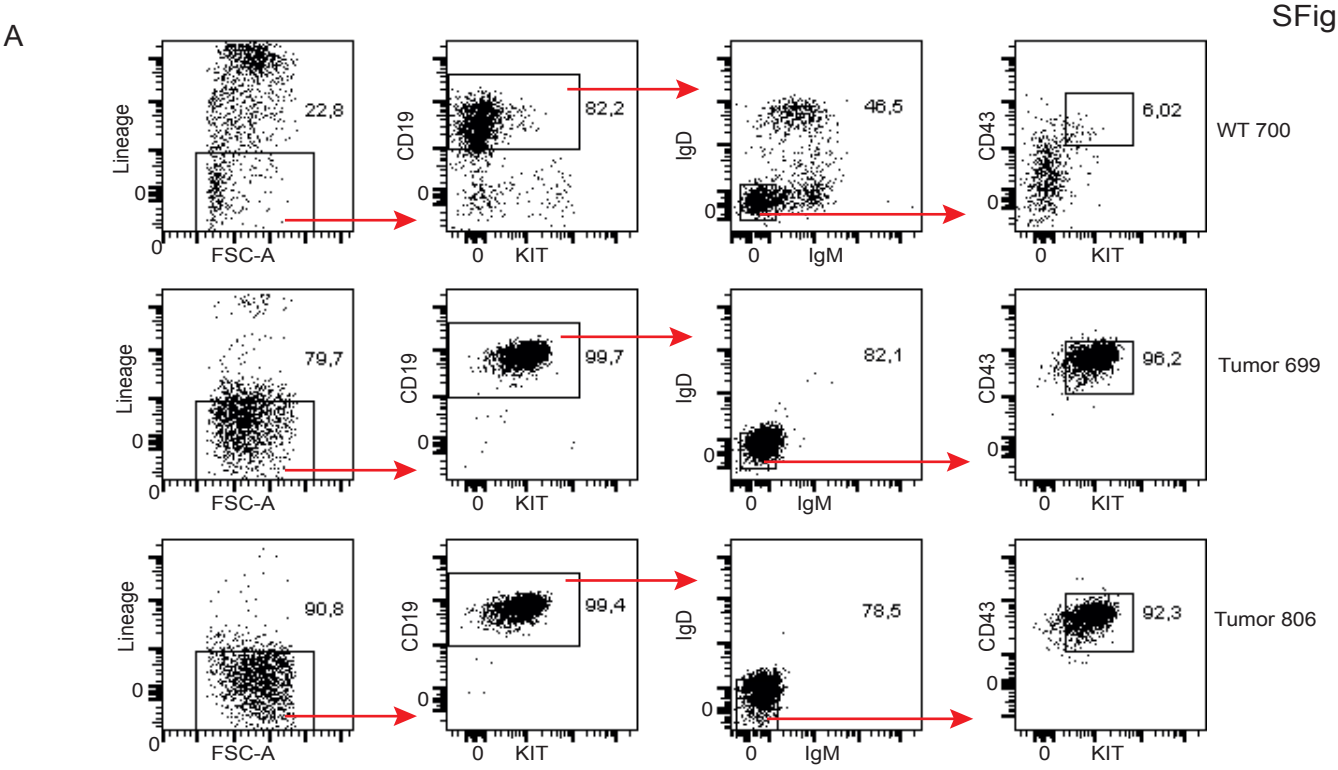
A
Lineage
FSC-A
22,8
CD19
KIT
82,2
IgD
IgM
46,5
CD43
KIT
6,02
WT 700
79,7
99,7
82,1
96,2
Tumor 699
90,8
99,4
78,5
92,3
Tumor 806

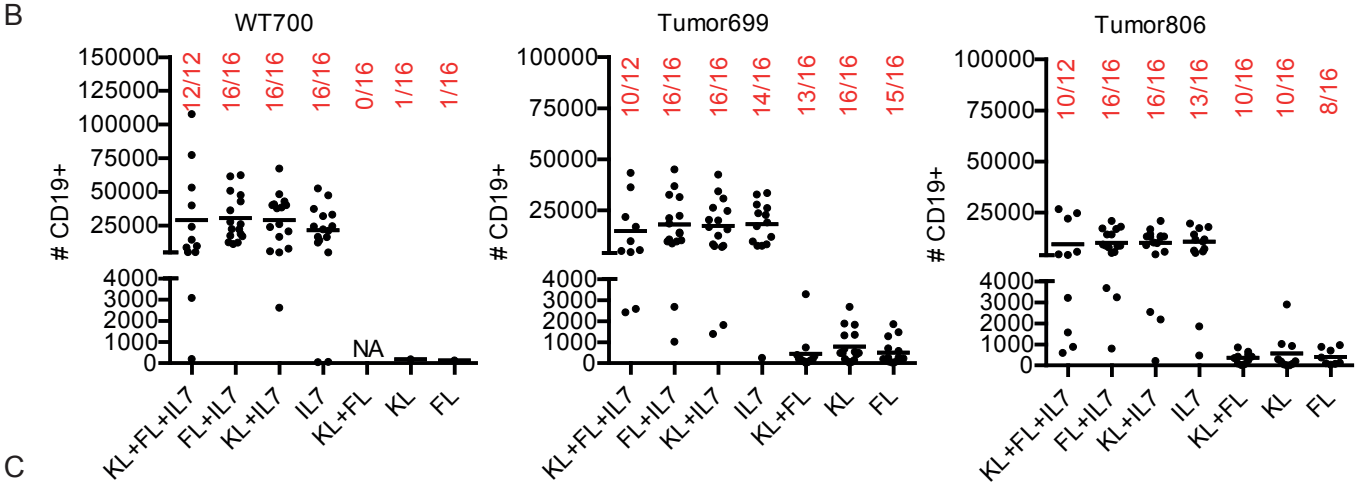
B
WT700
Tumor699
Tumor806
CD19+
12/12
16/16
16/16
16/16
0/16
1/16
1/16
10/12
16/16
16/16
14/16
13/16
16/16
15/16
10/12
16/16
16/16
13/16
10/16
10/16
8/16
NA
KL+FL+IL7
FL+IL7
KL+IL7
IL7
KL+FL
KL
FL

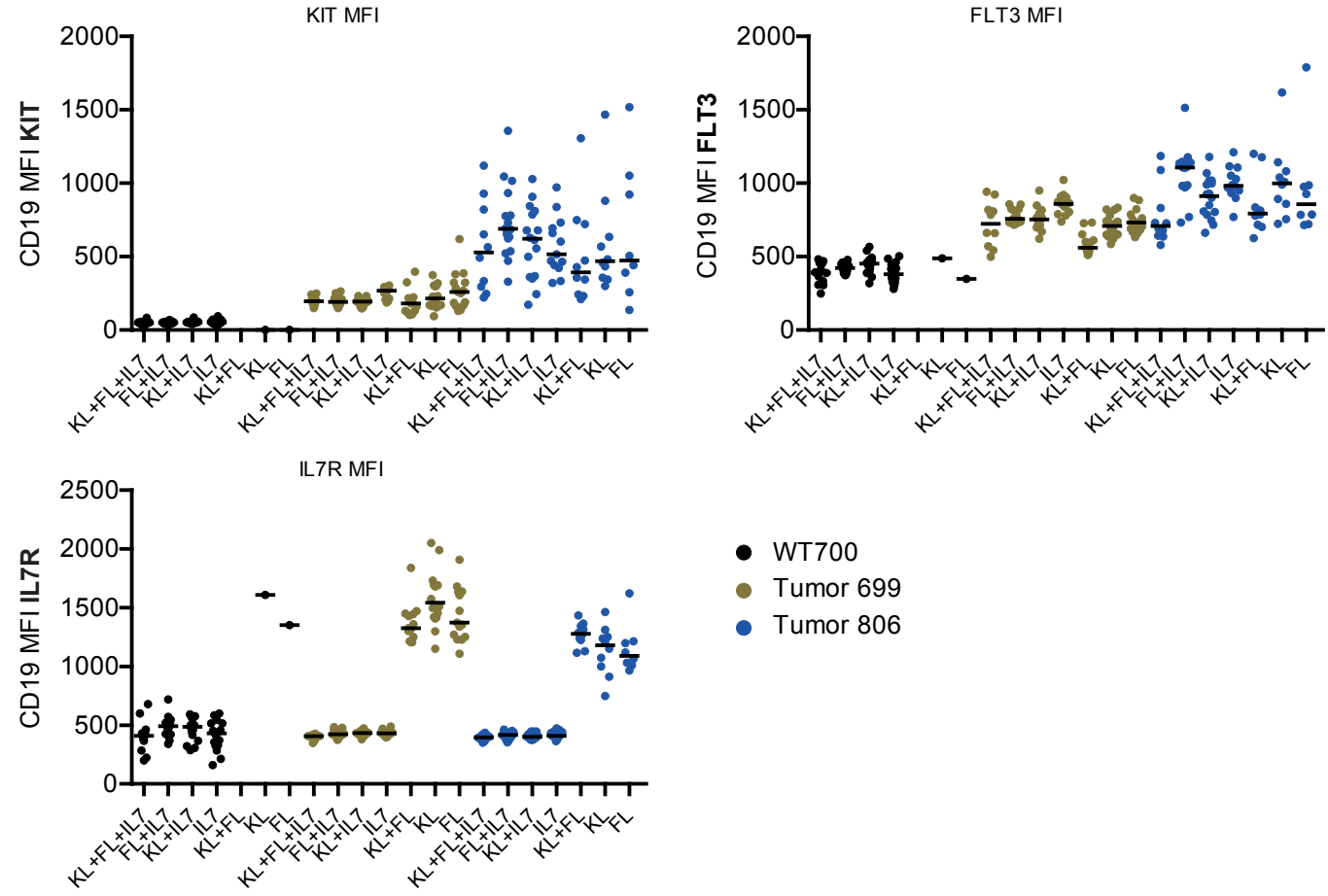
C
KIT MFI
FLT3 MFI
IL7R MFI
CD19 MFI KIT
CD19 MFI FLT3
CD19 MFI IL7R
WT700
Tumor 699
Tumor 806

Figure S3. IL7 can impact B-ALL growth *in vitro* and *in vivo*. A) Flow cytometry plots demonstrating the sorting strategy used for *in vitro* co-culture of OP9 stroma with *Wt* and tumor Pro-B cells. B) Graphs displaying the result of a 10-day *in vitro* OP9 stroma co-culture of sorted bone marrow Pro-B (500/well) ($LIN^-CD19^+IgM^-IgD^-CD43^+KIT^+$) from one *Wt* (700) and two leukemic (699, 806) mice. Text on x-axis represents the cytokine culture conditions, while numbers on y-axis are the total number of $CD19^+$ cells present in the well at analysis, based on counted events by flow cytometry during a fixed time of sample acquisition. Numbers in red are the number of positive wells / total number of seeded wells. C) Median fluorescence intensity (MFI) of analyzed $CD19^+$ cells with regard to surface expression of IL7R, FLT3 and KIT in the samples in B.

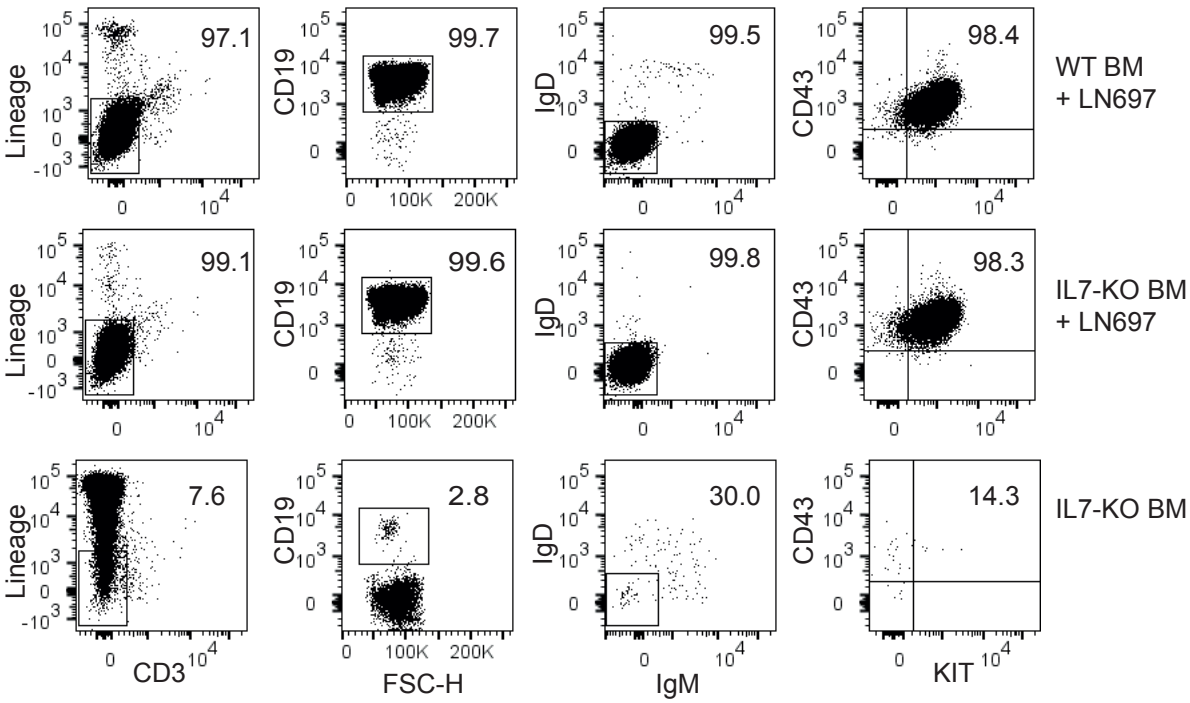
Lineage
CD19
IgD
CD43
97.1
99.7
99.5
98.4
WT BM
+ LN697
99.1
99.6
99.8
98.3
IL7-KO BM
+ LN697
7.6
2.8
30.0
14.3
IL7-KO BM
CD3
FSC-H
IgM
KIT

Figure S4: IL7 deficiency does not impact leukemia cell differentiation. Representative FACS plots showing the Pro-B profile in BM of *Wt.* (top) and *IL7*$^{-/-}$ (middle) recipients transplanted with tumor cells (#697) and the appearance of a normal *Il7*$^{-/-}$ BM (bottom). Lineage indicate CD19^{-} Linage positive cells.

Experimental procedures

Animal models.

Heterozygote *Pax5*$^{+/-}$ and *Ebf1*$^{+/-}$ mice were crossed to generate *Pax5*$^{+/-}$ *Ebf1*$^{+/-}$ mice (1). *Pax5*$^{+/-}$ *Ebf1*$^{+/-}$ and *Il7*$^{-/-}$ (2) mice were on C57BL/6 (CD45.2) background. Adoptive transfers were performed by tail vein injection of 100 000 sorted primary tumor cells to 12-16 weeks old mice in PBS/1%iFCS to CD45.1^{+} C57BL/6 non-conditioned animals. Disease was manifested by palpable accessory axillary- or subiliac- lymphnodes (LN) (3) and splenomegaly within 3-4 weeks after transplantation (1). Animal procedures were performed with consent from the local ethics committee at Linköping University (Linköping, Sweden).

Fluorescence Activated Cell Sorting (FACS).

Samples were subjected to red blood cell lysis by ice cold erythrocyte lysis buffer (150 mM NH_4Cl, 10 mM $NaHCO_3$, 1 mM EDTA) before staining. For analysis and cell sorting of B lineage cells from BM, spleen and LN´s, CD16/CD32 (FC) –blocked (93, eBioscience, SanDiego CA) cells were stained with antibodies against lineage markers CD11b/Mac1 (M1/70), Gr1 (RB6-8C5), TER119 (Ter119), CD3 (17A2, BD Pharmingen), CD11c (N418) and NK1.1 (PK136) and CD19 (ID3), CD43 (S7), KIT (2B8), IgM (RMM-1) and IgD (11-26. eBioscience). Samples from transplanted mice were analyzed using antibodies against CD45.1 (A20), CD45.2 (104) in addition to the panels presented above, or any of the following panels to identify specific populations. NK1.1 (PK136), CD3 (17A2), CD19 (ID3), GR1 (RB6 8C5), CD11b/Mac1 (M1/70).

Isolation of BM mononuclear cells for stroma analysis was performed as previously described (4, 5) while the isolation of non-hematopoietic cells in the spleen was based on expression of

MHC class I (MHC1^{+}) lack of MHC class II (MHCII) and expression or lack of expression of CD31 to discriminate between endothelial (CD31^{+}) and stoma cells (CD31^{-}).

Next generation sequencing and data analysis.

Total RNA for RNA-sequencing was isolated from sorted MSC, MPC CD51^{-}SCA1^{-}, CD44^{+} and ProB cells using RNAeasy Micro Kit (Qiagen, Hilden, Germany). Libraries were constructed using NuGEN's Ovation Ultralow Library systems (NuGEN Technologies, San Calros, CA) and were subjected to 76 cycles of sequencing on a NextSeq500 (Illumina, San Diego, CA). Quality check was performed using FastQC https://www.bioinformatics.babraham.ac.uk/projects/fastqc/. Overrepresented sequences were excluded and low quality bases were removed by trimmomatic/0.36 using SLIDINGWINDOW 5:20 MINLEN:35. Reads were mapped to mouse genome mm10 (GRCm38.p4) using STAR (6) and annotated by featureCounts (http://subread.sourceforge.net). Low expressing genes with a read MAX<40 across all samples, were filtered out and differentially expressed genes were identified using DESeq2 (7) for *R* using an FDR p-value of <0.05 with 2-fold change cut off. Heat maps were finalized by hierarchical clustering of DESeq2 normalized reads in Cluster3 (8) followed by visualization in Java Treeview (9). Gene expression heat maps were clustered using Log transformation, center genes on means and average linkage (uncentered correlation) hierarchical clustering of genes and arrays. Principal component analysis (PCA) was performed in R using the plotPCA function.

In silico analysis of receptor ligand interaction.

In order to identify receptor ligand pairs we explored the databases; KEGG (https://www.genome.jp/kegg/), DIP (http://dip.mbi.ucla.edu/dip/), HPMR (http://www.receptome.org/), IUPHAR (http://www.guidetopharmacology.org/), and HPRD

(http://www.hprd.org/). Putative receptor ligand pairs identified were searched on the STRING database (https://string-db.org/) to identify experimentally confirmed interactions. This generated a list consisting of 1,700 verified receptor ligand pairs and the genes encoding the proteins were identified. Genes expressed in each cell lineage were identified by RNA-seq with cut-off of ≥ 40 read counts. Gene lists of hematopoietic and BM stromal cells were processed side by side with receptor-ligand pairs on an excel file to identify and extract putative interactions; when a proper receptor for a ligand from donor cells was discovered on acceptor cells, the pair was classified as true and listed.

In vitro analysis of population dynamics and gene induction in stroma cells.

Normal wild type (*Wt*) or tumor ProB cells were plated at a concentration of 1-500 cells per well in 96 well plates containing pre-plated OP9 stroma cells. Cultures were kept in OptiMEM supplemented with 10% heat-inactivated fetal calf serum (FCS), 50μg/mL Gentamicin, and 50μM β-mercaptoethanol and 0-10ng/mL KIT ligand, 0-10ng/mL Fms-like tyrosine kinase 3 ligand (FLT3L), 0-10ng/mL interleukin-7. All cytokines were acquired from Peprotech (Rocky Hill, NJ). Cultures were substituted with fresh cytokines after 7 days. Cell cultures were analyzed by FACS at day 10 and stained against CD19 (1D3, eBioscience), FLT3, IL7R and KIT (BioLegend SanDiego CA). Cell expansion in cultures was determined by FACS by counting the number of events recorded from 70 μL of sample during a 20 second period at a fixed speed.

To explore the cellular response of stroma cells to leukemia *in vitro*, 500 000 primary B-ALL cells were incubated together with OP9 stroma cells in the presence of FLT3L (10ng/mL), IL7 (10 ng/mL) and KIT (10 ng/mL) as above. After five days of co-culture, CD45$^-$ cells were sorted and subject to Q-PCR analysis as above.

Data sharing.

The gene expression data can be found at GEO with accession number GSE118964 and the remaining data can be obtained from the corresponding author (MS).

References:

1. Prasad MA, Ungerback J, Ahsberg J, Somasundaram R, Strid T, Larsson M, et al. Ebf1 heterozygosity results in increased DNA damage in pro-B cells and their synergistic transformation by Pax5 haploinsufficiency. Blood. 2015 Jun 25;125(26):4052-9.

2. von Freeden-Jeffry U, Vieira P, Lucian LA, McNeil T, Burdach SE, Murray R. Lymphopenia in interleukin (IL)-7 gene-deleted mice identifies IL-7 as a nonredundant cytokine. J Exp Med. 1995;181(4):1519-26.

3. Van den Broeck W, Derore A, Simoens P. Anatomy and nomenclature of murine lymph nodes: Descriptive study and nomenclatory standardization in BALB/cAnNCrl mice. J Immunol Methods. 2006 May 30;312(1-2):12-9.

4. Qian H, Badaloni A, Chiara F, Stjernberg J, Polisetti N, Nihlberg K, et al. Molecular characterization of prospectively isolated multipotent mesenchymal progenitors provides new insight into the cellular identity of mesenchymal stem cells in mouse bone marrow. Mol Cell Biol. 2013 Feb;33(4):661-77.

5. Xiao P, Dolinska M, Sandhow L, Kondo M, Johansson AS, Bouderlique T, et al. Sipa1 deficiency-induced bone marrow niche alterations lead to the initiation of myeloproliferative neoplasm. Blood Adv. 2018 Mar 13;2(5):534-48.

6. Dobin A, Davis CA, Schlesinger F, Drenkow J, Zaleski C, Jha S, et al. STAR: ultrafast universal RNA-seq aligner. Bioinformatics. 2013 Jan 1;29(1):15-21.

7. Love MI, Huber W, Anders S. Moderated estimation of fold change and dispersion for RNA-seq data with DESeq2. Genome biology. 2014;15(12):550.

8. de Hoon MJ, Imoto S, Nolan J, Miyano S. Open source clustering software. Bioinformatics. 2004 Jun 12;20(9):1453-4.

9. Saldanha AJ. Java Treeview--extensible visualization of microarray data. Bioinformatics. 2004 Nov 22;20(17):3246-8.